Carbohydrate Polymers 81 (2010) 182–187

Contents lists available at ScienceDirect

Carbohydrate Polymers

journal homepage: www.elsevier.com/locate/carbpol

Effect of cupric ion on thermal degradation of quaternized chitosan

Si-Dong Li [a], Chao-Hua Zhang [b], Jing-Jing Dong [a], Chun-Yan Ou [a], Wei-Yan Quan [a], Lei Yang [a,*], Xiao-Dong She [a]

[a] College of Science, Guangdong Ocean University, Zhanjiang 524088, PR China
[b] College of Food Science and Technology, Guangdong Ocean University, Zhanjiang 524088, PR China

ARTICLE INFO

Article history:
Received 10 August 2009
Received in revised form
23 November 2009
Accepted 5 February 2010
Available online 10 March 2010

Keywords:
Hydroxypropyl trimethyl ammonium chloride chitosan
Cupric ion
Thermal degradation
Thermogravimetry analysis
Differential thermal analysis

ABSTRACT

The thermal degradation of quaternized chitosan–cupric ion compounds in nitrogen was studied by thermogravimetry analysis (TG) and differential thermal analysis (DTA). The effect of cupric ions on the thermal degradation behaviors of quaternized chitosan was discussed. Fourier transform-infrared (FTIR) and X-ray diffraction (XRD) were utilized to determine the micro-structure of quaternized chitosan–cupric ion compounds. The results of FTIR and XRD show that there are coordinating bonds between quaternized chitosan and cupric ions. Thermal analysis indicates that the thermal degradation of quaternary chitosan–cupric ion compounds is a two-stage reaction, in which there are the decomposition of N–C2 bond on the side-chain of quaternized chitosan and the cleavage of glycosidic linkages of chitosan. The two reactions are exothermic. The impact of cupric ion on the thermal degradation of quaternized chitosan is significant, and the temperature and activation energy of the degradation are related to the weight fraction of the cupric ion.

1. Introduction

Chitosan (CS), the second most abundant natural polysaccharide after cellulose, is produced by the deacetylation of chitin, and comes mainly from the by-product of the fishing industry (Varma, Deshpande, & Kennedy, 2004). Chitosan is widely used in medical, biological engineering, food and other industries, because of its excellent properties such as non-toxicity, biocompatibility and biodegradability (Kofuji, Murata, & Kawashima, 2005; Xi & Wu, 2004). But the application of chitosan is limited owing to its insolubility in water (Ma et al., 2008).

Currently, many studies to prepare derivatives of chitosan by chemical modifications in order to increase the solubility in water have been reported, and most are about introduction of some hydrophilic substituent by chemical modification which resulted in improvement of solubility (Chung, Kuo, & Chen, 2005; Lim & Hudson, 2003). Various water-soluble chitosan derivatives are prepared by alkylation (Sajomsang, Tantayanon, Tangpasuthadol, & Daly, 2008), carboxymethylation (Chen & Park, 2003), quaternization (Lim & Hudson, 2004), and the quaternized derivative of chitosan is attracted most attention. Caiqin Qin (Qin et al., 2004) prepared chitosan-*N*-2-hydroxypropyl trimethyl ammonium chloride, and demonstrated that it had good solubility in water. Yajun Xie (Xie, Liu, & Chen, 2007) obtained chitosan derivative with better solubility by quaternization. Water solubility is of great importance for chitosan of its antibacterial activity. Biological activity of chitosan is limited because its poor solubility only when the pH of solution is above 6.5. But quaternary ammonium chitosan, that is quaternized derivative of chitosan, is freely soluble over a wide pH range, and exhibited better water solubility and stronger antibacterial activity than chitosan (Lim & Hudson, 2003). The water-soluble quaternary ammonium salts of chitosan are soluble in both acidic and basic physiological circumstances, so they might be good candidates as polycationic antiseptics, and the quaternary ammonium chitosan is more widely used in antibacterial, anti-oxidation, and related applications than chitosan.

The flexibility of the material, insolubility in the vast majority of solvents, but capability of being cast into films and fibres from dilute acid, along with its inherent chirality make chitosan an excellent candidate as a support for catalysis (Tong, Li, & Xia, 2005). In recent years, polymer–metal complexes have attracted much attention for its high catalytic activity and selectivity. An amino group in C2 and a hydroxyl group in C3 on its pyranose ring which are both of equatorial bonds, allow chitosan to chelate metal ions over a certain pH range. CS has stable coordination to cupric ion, and its complex (CS-Cu) is stable in the organic solvent, which could serve as an initiator for vinyl monomer such as methyl methacrylate and acrylonitrile in the presence of carbon tetrachloride (Inaki, Otsuru, & Takemoto, 1978). CS-Pd and CS-Co also could be catalyst for organic reactions with high catalysis (Tong et al., 2005; Yi,

* Corresponding author. Tel.: +86 13822588001; fax: +86 759 2383636.
E-mail address: yanglei2218@yahoo.com.cn (L. Yang).

0144-8617/$ – see front matter © 2010 Elsevier Ltd. All rights reserved.
doi:10.1016/j.carbpol.2010.02.049

Lee, Sin, & Lee, 2007). Recently, it is reported that a quaternary ammonium salt covalently bound to chitosan is an efficient and recyclable single-component catalyst for the synthesis of propylene carbonate (Zhao et al., 2007). For use as a catalyst thermal stability is of most importance, but there are, unfortunately, few reports about the impact of cupric ion on the thermal stability of quaternary ammonium salts of chitosan. In this paper, hydroxypropyl trimethyl ammonium chloride chitosan (HTCC) with better water solubility, was synthesized through using CS as raw material and epoxypropyl trimethyl ammonium chloride (ETA) as a grafting agent. Then hydroxypropyl trimethyl ammonium chloride chitosan–cupric ion compound samples were obtained by mixing water solution of cupric sulfate with chitosan solution in 1% acetic acid, casting and drying. Furthermore, Fourier transform-infrared (FTIR) and X-ray diffraction (XRD) analysis are utilized to determine the micro-structure of quaternized chitosan–cupric ion compounds. The thermal degradation of HTCC in the existence of cupric ion is studied by using thermogravimetric analysis (TG) and differential thermal analysis (DTA), and the thermal degradation mechanism of chitosan is discussed.

2. Experimental

2.1. Materials

Chitosan was obtained by Shanghai Greenbird Science and Technology Development Company (Shanghai, China), its viscosity average molecular weight was 1.8×10^5, and the degree of deacetylation of chitosan was more than 90%.

2.2. Preparation of hydroxypropyl trimethyl ammonium chloride chitosan (Huang, Chen, Sun, Hu, & Gao, 2006; Lang, Wendel, & Konrad, 1990)

CS and ETA were accurately weighted, added 15 mL isopropyl alcohol and 45 mL distilled water, stirred at 85 °C for 10 h. The final products (HTCC) were obtained, sedimented by acetone, washed by methanol and acetone/alcohol (v/v = 4:1), filtered and dried, respectively.

2.3. Determination of degree of substitution (Li, Du, Wu, & Zhang, 2004)

0.2 g of quaternary chitosan was dissolved into 100 mL distilled water. Then 25 mL of this as-prepared solution was extracted into a beaker and 25 mL distilled water was complemented, followed by adding sodium hydroxide to adjust the pH of reacting solution to 8.6–9.2. And the solution of quaternary chitosan is titrated by 0.1 mol L^{-1} silver nitrate solution, 1 mL 5% potassium chromate as indicator. The degree of substitution (DS) is calculated as follows:

$$\mathrm{DS} = \frac{V \times c \times 10^{-3}}{V \times c \times 10^{-3} + (W - V \times c \times 10^{-3} \times 314)/162} \times 100\%$$

where V (mL) is the volume of $AgNO_3$ solution, C (mol L^{-1}) is the concentration of $AgNO_3$ solution, W (g) is the weight of HTCC, 314 (mol g^{-1}) is the molar mass of quaternary chitosan and 162 (mol g^{-1}) is the molar mass of glucosamine.

2.4. Preparation of hydroxypropyl trimethyl ammonium chloride chitosan–cupric ion compounds

The hydroxypropyl trimethyl ammonium chloride chitosan–cupric ion compound samples were obtained by mixing cupric sulfate solution with hydroxypropyl trimethyl ammonium chloride chitosan solution in 1% acetic acid, casting and drying. The samples were transparent homogeneous films containing 0–4% weight fraction of cupric ion, for Sample 1, pure hydroxypropyl trimethyl ammonium chloride chitosan, Sample 2, Cu^{2+}/HTCC = 0.5%, Sample 3, Cu^{2+}/HTCC = 1%, Sample 4, Cu^{2+}/HTCC = 2%, Sample 5, Cu^{2+}/HTCC = 4%, respectively.

2.5. FTIR analysis

A Perkin-Elmer Spectrum 100 infrared spectrometer was used to obtain FTIR data. FTIR spectra were recorded in the wave number range of 4000–400 cm^{-1} with a resolution of 4 cm^{-1}.

2.6. X-ray diffraction analysis

X-ray diffraction patterns of samples were measured by a D/max IIIA diffractometer (Rigaku, Japan) and used a Cu K_α target at 35 kV and 25 mA.

2.7. Thermogravimetric analysis

Thermogravimetric analysis (TG) and differential thermal analysis were performed on Perkin-Elmer TG/DTA6300 system. The mass of each sample was 5–6 mg. The carrier gas was nitrogen at a flow rate of 50 mL min^{-1}. The samples were heated from 30 to 600 °C with the heating rate (u) of 10 °C min^{-1} to record the TG, differential thermogravimetric analysis (DTG) and DTA curves.

2.8. Data processing

The kinetic parameters of a thermal decomposition reaction can be evaluated by dynamic experiments. In this case, the sample is heated from room temperature until its complete decomposition at a linearly programmed rate. In thermogravimetric measurements, the extent of decomposition can be calculated as follows:

$$\alpha = \frac{W_0 - W_t}{W_0 - W_f} \tag{1}$$

where α is extent of decomposition; W_t, W_0 and W_f are the actual, initial, and final mass of the sample, respectively. A typical model for a kinetic process can be expressed as:

$$-\frac{d(1-\alpha)}{dt} = kf(\alpha) \tag{2}$$

where $-d(1-\alpha)/dt$ is the decomposition rate; $f(\alpha)$, the function of α, depends on the particular decomposition mechanism, the simplest and the most frequently used model of that is:

$$f(\alpha) = (1-\alpha)^n \tag{3}$$

where n is the reaction order.

k is the decomposition rate constant, which is assumed to obey the Arrhenius relationship:

$$k = Ae^{-E_a/RT} \tag{4}$$

where A is the preexponential factor (s^{-1}), E_a is the activation energy (J mol^{-1}), R is the gas constant (8.314 J mol^{-1}) and T is the absolute temperature (K). Substituting Eqs. (4) and (3) into Eq. (2), we obtain

$$-\frac{d(1-\alpha)}{dt} = Ae^{-E_a/RT}(1-\alpha)^n \tag{5}$$

When a dynamic experiment is performed, the temperature T, changes linearly from the initial temperature T_0, according to the heating rate u, during the time t, then:

$$T = T_0 + ut \tag{6}$$

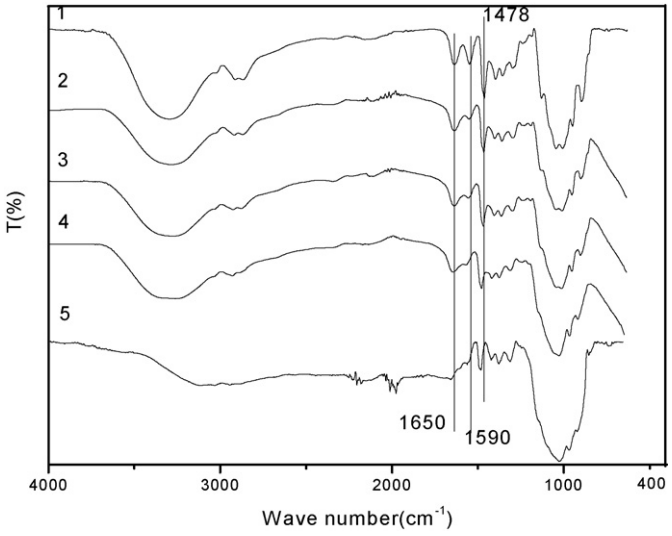

Fig. 1. FTIR spectra of quaternary chitosan and quaternary chitosan–cupric ion compounds.

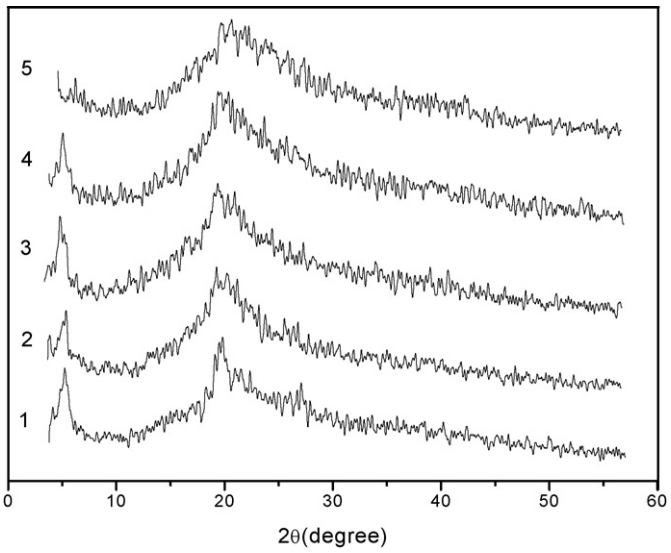

Fig. 2. X-ray diffraction patterns of quaternary chitosan and quaternary chitosan–cupric ion compounds.

Eqs. (5) and (6) may be combined to give:

$$\frac{d(1-\alpha)}{(1-\alpha)_n} = \frac{A}{u} e^{-E_a/RT} dT \tag{7}$$

This, according to Broido (1969), can be expressed as:

$$\ln\left[ln\left(\frac{1}{1-\alpha}\right)\right] = -\frac{E_a}{RT} + \ln\left[\left(\frac{R}{E_a}\right)\left(\frac{Z}{u}\right)T_M^2\right] \tag{8}$$

where T_m is the temperature of the maximum reaction velocity and Z is a constant, the activation energy is determined from the slope of the straight line which results by plotting $\ln\{\ln[1/(1-\alpha)]\}$ versus $1/T$.

3. Results and discussion

3.1. FTIR analysis

FTIR spectra of quaternized chitosan and quaternized chitosan–cupric ion compounds are shown in Fig. 1. For quaternized chitosan (Sample 1), a strong and broad absorbent band centered at 3297 cm^{-1} is attributed to –OH asymmetrical stretching vibration and $-NH_2$ stretching vibration (Sajomsang, Gonil, & Tantayanon, 2009). There is a sharp increase of intensity of the band near 2960–2850 cm^{-1}, which is attributed to C–H stretching of the alkyl substituent (de Britto & de Assis, 2007). The absorption bands at 1650 and 1590 cm^{-1} are assigned as amide I and amide II vibrations, respectively. The band at 1412 cm^{-1} is attributed to bending vibration of –C–N–, while band at 1028 cm^{-1} is to –C–O–C– bending vibration (Vachoud, Chen, Payne, & Vazquez-Duhalt, 2001). Compared with chitosan (Ou et al., 2008), the absorption band at 1478 cm^{-1}, which corresponds to an asymmetric angular bending of methyl groups (Jia, Shen, & Xu, 2001; Li et al., 2004; Mi, Shyu, Chen, & Schoung, 1999), shows the introduction of the quaternary ammonium salt group on chitosan backbone. For quaternized chitosan–cupric ion compounds (Samples 2–5), the wide absorption band at 3297 cm^{-1} corresponds to the stretching vibration of NH_2 group and OH group, a significant decrease of wave numbers is observed along with the increasing of weight fraction of cupric ion (3293–3102 cm^{-1}), which contributes to the effect of ETA (Sun & Wang, 2006). The bands at 1650 and 1590 cm^{-1} show a weaken absorption with the increase of cupric ions, for the interaction of $-NH_2$ in chitosan with cupric ion forming the quaternized chitosan–Cu(II) complex. It can be seen that the absorption wave numbers of –C–O–C– stretching vibration of quaternized chitosan–cupric ion compounds are more than that of quaternized chitosan, which is taken as an evidence of the decrease of the bond energies of glycosidic linkage in chitosan, and quaternized chitosan–cupric ion compound is easier to degrade (Yin, Zhang, Yu, Yang, & Lin, 2002).

3.2. X-ray diffraction (XRD) analysis

Fig. 2 shows the X-ray diffraction patterns of quaternary chitosan and quaternary chitosan–cupric ion compounds. For quaternary chitosan (Sample 1), the XRD pattern exhibits two characteristic peaks at $2\theta = 4.5^\circ$ and 20.1° For quaternary chitosan–cupric ion compounds (Samples 2–5), it can be seen that the two characteristic peaks are gradually absent with the increasing of weight fraction of cupric ion incorporated in quaternary chitosan, and the crystallinity of Samples 1–5 also gradually decreases, 16.8%, 8.6%, 8.5%, 7.3% and 4.5%, respectively. The results indicate that the quaternary chitosan and cupric ion formed a complex because of the interaction of $-NH_2$ in chitosan with cupric ion, which leads to the decrease of the crystallinity of chitosan and its thermal stability (Ou et al., 2008).

3.3. Thermogravimetric analysis

The TG curves and the corresponding DTG curves of quaternary chitosan and quaternary chitosan–cupric ion compounds are shown in Fig. 3. It can be seen that there are three peaks on the DTG curves. The first peak appears around 100 °C, which is attributed to the evaporation of absorbed water in the inner polymer (López, Mere, Alguacil, & López-Delhado, 2008). So quaternary chitosan and quaternary chitosan–cupric ion compounds are degraded in two stages corresponding to the second peak and the third peak, respectively. The characteristic temperatures for the two stages of thermal degradation of quaternary chitosan and quaternary chitosan–cupric ion compounds are given in Table 1. T_{st} is the temperature of initial weight loss and T_{max} is the temperature at maximum weight loss rate, that is the peak temperature on a DTG curve.

The first thermal degradation process occurs in the temperature range (160–260 °C). For quaternary chitosan (Sample 1), it starts at 227 °C and reaches a maximum at 251 °C. For quaternary

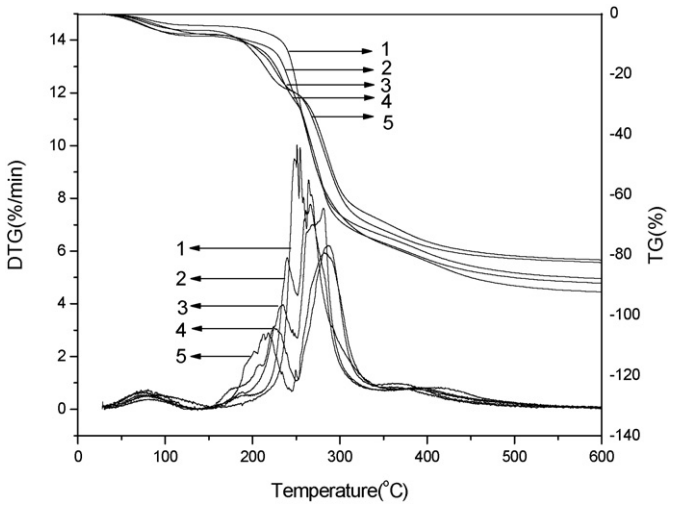

Fig. 3. TG and DTG curves of thermal degradation of quaternary chitosan and quaternary chitosan–cupric ion compounds.

Table 1
Characteristic temperatures for the thermal degradation of quaternary chitosan–cupric ion compounds.

Sample	The first stage (160–260 °C)		The second stage (260–350 °C)	
	T_{st} (°C)	T_{max} (°C)	T_{st} (°C)	T_{max} (°C)
1	227	251	–	265
2	216	240	–	267
3	212	234	–	281
4	197	225	–	287
5	186	224	–	289

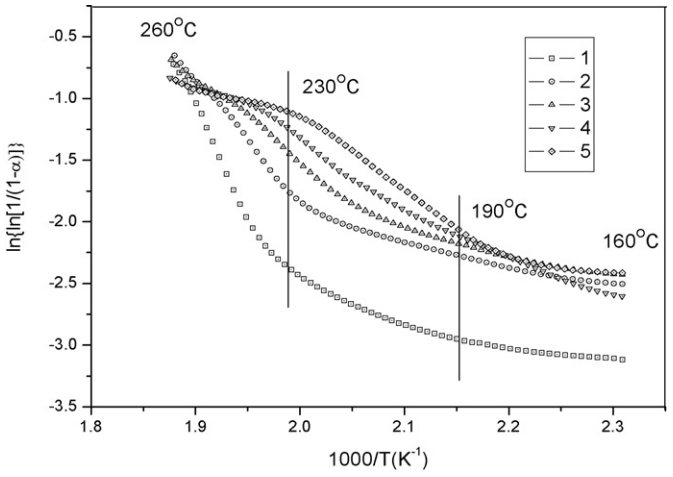

Fig. 4. The relationships between $\ln\{\ln[1/(1-\alpha)]\}$ and $1/T$ in the first thermal degradation stage of quaternary chitosan and quaternary chitosan–cupric ion compounds.

Table 3
The peak temperatures and heat effect on the DTA curves during the thermal degradation of quaternary chitosan–cupric ion compounds.

Sample	The first stage (160–260 °C)		The second stage (260–350 °C)	
	Peak temperature (°C)	Heat effect	Peak temperature (°C)	Heat effect
1	249	Exo	–	Exo
2	242	Exo	–	Exo
3	231	Exo	329	Exo
4	216	Exo	325	Exo
5	211	Exo	319	Exo

chitosan–cupric ion compounds (Samples 2–5), the temperature of initial weight loss (T_{st}) and the temperature of maximal weight loss rate (T_{max}) decrease along with increasing weight fraction of cupric ion (C), which can be expressed as follows: $T_{st} = -9.90C + 222 (R^2 = 0.938)$, and $T_{\max} = -8.61C + 246 (R^2 = 0.926)$, respectively.

The apparent activation energies (E_a) for the thermal degradation of quaternary chitosan and quaternary chitosan–cupric ion compounds in nitrogen are calculated from the TG curves using the method described by Broido. Broido method is based on Eq. (8). Plots of $\ln\{\ln[1/(1-\alpha)]\}$ versus $1/T$ for the temperature range 160–260 °C, which is in the first thermal degradation stage, are shown in Fig. 4.

It can be seen that there are three distinct degradation periods in the first thermal degradation stage. The E_a obtained for the three degradation periods are reported in Table 2. The results indicate that, the conformation change of quaternary chitosan resulted from the mixing of cupric ion in it has effect on the formation of new phases of the polymer, which partly decreases bond energies of glycosidic linkages in quaternary chitosan, consequently leads to its thermal instability. The decrease of E_a in the first thermal degradation stage is observed with increasing amount of cupric ion, and its thermal stability is also significantly declined. And the first thermal degradation is of vital importance for the thermal stability of the polymer.

The second thermal degradation process occurs in the temperature range (260–350 °C), where T_{max} increases along with increasing weight fraction of cupric ion (C) (Table 2). From plots of $\ln\{\ln[1/(1-\alpha)]\}$ versus $1/T$ in the second thermal degradation stage, it can be seen that there is two degradation periods. The E_a obtained for the two degradation periods are reported in Table 2. The results show that E_a increases along with increasing weight fraction of cupric ion.

3.4. Differential thermal analysis

DTA curves of quaternary chitosan and quaternary chitosan–cupric ion compounds recorded in nitrogen from 30 to 600 °C are shown in Fig. 5. Table 3 summarizes the heat effect data for the samples. For quaternary chitosan (Sample 1), the exothermic peak at 249 °C in the first stage (160–260 °C) corresponds to decomposition of N–C2 bond on the side-chain of quaternized chitosan (de Britto & Campana-Filho, 2004), and

Table 2
Activation energies during the two thermal degradation stages of quaternary chitosan–cupric ion compounds.

Sample	Stage 1 (160–260 °C)				Stage 2 (260–350 °C)		
	Period I (160–190 °C) E_a (kJ mol^{-1})	Period II (190–230 °C) E_a (kJ mol^{-1})	Period III (230–260 °C) E_a (kJ mol^{-1})	Total E_a (kJ mol^{-1})	Period I (260–305 °C) E_a (kJ mol^{-1})	Period II (305–350 °C) E_a (kJ mol^{-1})	Total E_a (kJ mol^{-1})
1	8.0	30.2	145.3	183.5	52.2	5.2	57.3
2	12.2	25.9	82.1	120.2	55.0	13.5	68.4
3	13.3	38.3	48.6	100.1	64.1	14.1	78.2
4	27.2	45.1	23.8	96.0	70.5	19.4	89.8
5	15.8	49.5	17.9	83.2	70.0	21.7	91.7

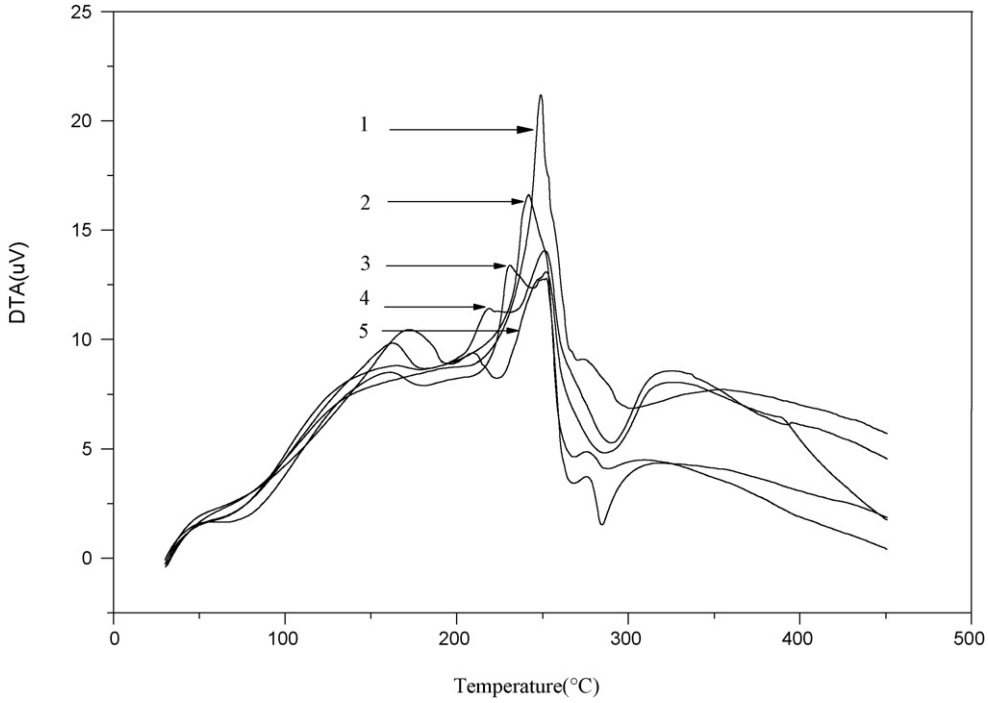

Fig. 5. DTA curves of thermal degradation of quaternary chitosan and quaternary chitosan–cupric ion compounds.

the second stage (260–350 °C) corresponds to the cleavage of glycosidic linkages of chitosan (Holme, Foros, Pettersen, Dornish, & Smidsord, 2001). For quaternary chitosan–cupric ion compounds (Samples 2–5), there are two exothermic peaks, and all peak temperatures shift to a lower temperature in two degradation stages with the increase of the amount of cupric ion, indicating that the chelating of chitosan with cupric ion leads to its thermal instability. These results are well correlated with the results of TG.

4. Conclusions

The thermal degradation of quaternary chitosan and quaternary chitosan–cupric ion compounds in nitrogen is a two-stage reaction, in which are the decomposition of N–C2 bond on the side-chain of quaternized chitosan and the cleavage of glycosidic linkages of chitosan. And the two reactions are exothermic. The effect of cupric ion on the thermal degradation of quaternized chitosan is significant, and the temperature of initial weight loss (T_{st}), the temperature of maximal weight loss rate (T_{max}), the peak temperature (T_p) on the DTA curve and the reaction activation energy (E_a) decrease along with increasing weight fraction of cupric ion.

References

Broido, A. (1969). A simple, sensitive graphical method of treating thermogravimetric analysis data. *Journal of Polymer Science, Part A-2*, *7*, 1761.

Chen, X. G., & Park, H. J. (2003). Chemical characteristics of O-carboxymethyl chitosans related to the preparation conditions. *Carbohydrate Polymers*, *53*, 355–359.

Chung, Y. C., Kuo, C. L., & Chen, C. C. (2005). Preparation and important functional properties of water-soluble chitosan produced through Maillard reaction. *Bioresource Technology*, *96*, 1473–1482.

de Britto, D., & Campana-Filho, S. P. (2004). A kinetic study on the thermal degradation of N,N,N-trimethylchitosan. *Polymer Degradation and Stability*, *84*, 353–361.

de Britto, D., & de Assis, O. B. G. (2007). Synthesis and mechanical properties of quaternary salts of chitosan-based films for food application. *International Journal of Biological Macromolecules*, *41*, 198–203.

Holme, H. K., Foros, H., Pettersen, H., Dornish, M., & Smidsord, O. (2001). Thermal depolymerization of chitosan chloride. *Carbohydrate Polymers*, *46*, 287–294.

Huang, R. H., Chen, G. H., Sun, M. K., Hu, Y. M., & Gao, C. J. (2006). Studies on nanofiltration membrane formed by diisocyanate cross-linking of quaternized chitosan on poly(acrylonitrile) (PAN) support. *Journal of Membrane Science*, *286*, 237–244.

Inaki, Y., Otsuru, M., & Takemoto, K. (1978). Vinyl polymerization by metal complexes-31. Initiation by chitosan–copper R(II) complex. *Journal of Macromolecular Science Chemistry*, *12*(7), 953–970.

Jia, Z. S., Shen, D. F., & Xu, W. L. (2001). Synthesis and antibacterial activities of quaternary ammonium salt of chitosan. *Carbohydrate Research*, *333*(1), 1–6.

Kofuji, K., Murata, Y., & Kawashima, S. (2005). Sustained insulin release with biodegradation of chitosan gel beads prepared by copper ions. *International Journal of Pharmaceutics*, *303*, 95–103.

Lang, G., Wendel, H., & Konrad, E. (1990). Process for making quaternary chitosan derivatives for cosmetic agents. *U.S. Patent 4921949*.

Li, H. B., Du, Y. M., Wu, X. J., & Zhang, H. Y. (2004). Effect of molecular weight and degree of substitution of quaternary chitosan on its adsorption and flocculation properties for potential retention-aids in alkaline papermaking. *Colloids and Surfaces A – Physicochemical and Engineering Aspects*, *242*, 1–8.

Lim, S. H., & Hudson, S. M. (2003). Review of chitosan and its derivatives as antimicrobial agents and their uses as textile chemicals. *Journal of Macromolecular Science – Polymer Reviews*, *C43*(2), 223–269.

Lim, S. H., & Hudson, S. M. (2004). Synthesis and antimicrobial activity of a water-soluble chitosan derivative with a fiber-reactive group. *Carbohydrate Research*, *339*, 313–319.

López, F. A., Mere, A. L. R., Alguacil, F. J., & López-Delhado, A. (2008). A kinetic study on the thermal behaviour of chitosan. *Journal of Thermal Analysis and Calorimetry*, *91*(2), 633–639.

Ma, G. P., Yang, D. Z., Zhou, Y. S., Xiao, M., Kennydy, J. F., & Nie, J. (2008). Preparation and characterization of water-soluble N-alkylated chitosan. *Carbohydrate Polymers*, *74*, 121–126.

Mi, F. L., Shyu, S. S., Chen, C. T., & Schoung, J. Y. (1999). Porous chitosan microsphere for controlling the antigen release of Newcastle disease vaccine: Preparation of antigen-adsorbed microsphere and in vitro release. *Biomaterials*, *20*(17), 1603–1612.

Ou, C. Y., Ii, S. D., Li, C. P., Zhang, C. H., Yang, L., & Chen, C. P. (2008). Effect of cupric ion on thermal degradation of chitosan. *Journal of Applied Polymer Science*, *109*, 957–962.

Qin, C. Q., Xiao, Q., Li, H. R., Fang, M., Liu, Y., Chen, X. Y., et al. (2004). Calorimetric studies of the action of chitosan-N-2-hydroxypropyl trimethyl ammonium chloride on the growth of microorganisms. *International Journal of Biological Macromolecules*, *34*, 121–126.

Sajomsang, W., Gonil, P., & Tantayanon, S. (2009). Antibacterial activity of quaternary ammonium chitosan containing mono or disaccharide moieties: Preparation and characterization. *International Journal of Biological Macromolecules*, *44*, 419–427.

Sajomsang, W., Tantayanon, S., Tangpasuthadol, V., & Daly, W. H. (2008). Synthesis of methylated chitosan containing aromatic moieties: Chemoselectivity and effect on molecular weight. *Carbohydrate Polymers*, *72*, 740–750.

Sun, S. L., & Wang, A. Q. (2006). Adsorption properties of carboxymethyl-chitosan and cross-linked carboxymethyl-chitosan resin with Cu(II) as template. *Separation and Purification Technology*, *49*, 197–204.

Tong, J. H., Li, Z., & Xia, C. G. (2005). Highly efficient catalysts of chitosan-Schiff base Co(II) and Pd(II) complexes for aerobic oxidation of cyclohexane in the absence of reductants and solvents. *Journal of Molecular Catalysis A: Chemical*, *231*, 197–203.

Vachoud, L., Chen, T. H., Payne, G. F., & Vazquez-Duhalt, R. (2001). Peroxidase catalyzed grafting of gallate esters onto the polysaccharide chitosan. *Enzyme and Microbial Technology*, *29*(6–7), 380–385.

Varma, A. J., Deshpande, S. V., & Kennedy, J. F. (2004). Metal complexation by chitosan and its derivatives: A review. *Carbohydrate Polymers*, *55*, 77–93.

Xi, F. N., & Wu, J. M. (2004). Macroporous chitosan layer coated on non-porous silica gel as a support for metal chelate affinity chromatographic adsorbent. *Journal of Chromatography A*, *1057*, 41–47.

Xie, Y. J., Liu, X. F., & Chen, Q. (2007). Synthesis and characterization of water-soluble chitosan derivate and its antibacterial activity. *Carbohydrate Polymers*, *69*, 142–147.

Yi, S. S., Lee, D. H., Sin, E., & Lee, Y. S. (2007). Chitosan-supported palladium(0) catalyst for microwave-prompted Suzuki cross-coupling reaction in water. *Tetrahedron Letters*, *48*, 6771–6775.

Yin, X. Q., Zhang, Q., Yu, W. X., Yang, L. C., & Lin, Q. (2002). Formation of chitosan Cu(II) complex and control degradation. *Chinese Journal of Inorganic Chemistry*, *18*(1), 87–90.

Zhao, Y., Tian, J. S., Qi, X. H., Han, Z. N., Zhuang, Y. Y., & He, L. N. (2007). Quaternary ammonium salt-functionalized chitosan: A easily recyclable catalyst for efficient synthesis of cyclic carbonates from epoxides and carbon dioxide. *Journal of Molecular Catalysis A: Chemical*, *271*, 284–289.